Environ. Sci. Technol. **2000**, *34,* 3632−3640

Macromolecular Characteristics of Natural Organic Matter. 2. Sorption and Desorption Behavior

EUGENE J. LEBOEUF*,† AND WALTER J. WEBER, JR.‡

Department of Civil and Environmental Engineering, Vanderbilt University, Nashville, Tennessee 37235, and Department of Civil and Environmental Engineering, The University of Michigan, Ann Arbor, Michigan 48109-2125

The effects of the relative macromolecular mobilities of natural organic matter (NOM) matrices on their sorption/desorption behavior with respect to phenanthrene are described. Sorption isotherm characteristics are found to correspond directly to the relative dominance of glassy and rubbery states, with nonlinear sorption being linked to the dominance of glassy regions within the natural and synthetic macromolecules examined. The Dual Reactive Domain Model (DRDM) developed in earlier studies provides an effective tool for identifying specific *ad*sorption and *ab*sorption contributions to overall isotherm patterns. The Hysteresis Index (H.I.), also developed in earlier studies, is useful for quantifying differences between the sorption and desorption isotherms for each macromolecular sorbent. Confirming earlier observations with soils and sediments, a trend of increasing H.I. with decreasing oxygen/carbon (O/C) atomic ratio is generally observed for the NOMs investigated. Correlation of isotherm nonlinearity and H.I. with macromolecular mobility is hypothesized and tested, leading to a general conclusion that the extent of isotherm nonlinearity and the H.I. are related to increasing glass transition temperature (T_g) of the NOM. Macromolecular sorbents display little or no desorption hysteresis under experimental conditions at or very near their T_g, while sorbents that are clearly in their glassy state under those conditions manifest significant desorption hysteresis. This may relate in part to the fact that the times required for attainment of true sorption and/or desorption equilibria vary with the mobility and flexibility of macromolecular sorbent matrices, attaining only over extremely long periods of solute migration into and out of the less flexible glassy states of such matrices.

Introduction

Regardless of the technology used, active remediation of chemically contaminated soils and sediments generally requires desorption of the contaminants of concern. Desorption of hydrophobic organic chemicals (HOCs) has frequently been observed to manifest apparent hysteresis (*1*−*14*). This hysteresis is often attributed to the occurrence of specific chemical reactions (e.g., formation of hydrogen or covalent bonds) between polar organic chemicals and polar sites on geosorbent surfaces (*8*, *11*, *13*, *15*). Recent work (*12*−*14*), however, has shown that desorption distribution coefficients for the relatively nonpolar and hydrophobic contaminant phenanthrene, for which only weak, physical binding with soil and sediment surfaces is expected, can be as much as 25% larger than corresponding sorption coefficients, implying that other mechanisms may be contributing to the observed hysteretic behavior.

Experimental artifacts can often play significant roles in generating apparent hysteresis behavior. A thorough study of this issue by Huang et al. (*12*) identified several sources of experimental artifacts on apparent desorption hysteresis, including (i) nonequilibrium effects resulting from use of equilibration periods too short to allow equilibrium to attain in either the sorption cycle, desorption cycle, or both cycles of the experiment; (ii) losses of solute to reactor system components; and (iii) solids concentration effects in which a portion of the solute partitions to a third phase (dissolved organic matter in solution). The results from these studies suggest that the flame-sealed ampule technique described by Ball and Roberts (*16*) may best be employed to reduce these sources of artifactual hysteresis.

Desorption studies by Harmon and Roberts (*17*), Huang et al. (*12*), and Weber et al. (*13*) using the flame-sealed ampule technique have revealed the existence of nonartifactual desorption hysteresis. Harmon and Roberts (*17*) and Farrell and Reinhard (*18*) have attributed such behavior to sorption within micropores present in mineral or organic matter fractions of soils and sediments. As often observed for the physical adsorption of gases by microporous solids, micropores on the order of a few sorbate molecules in diameter may possess overlapping potential fields from neighboring micropore walls, allowing for increased energies of interaction between sorbate and sorbent (*19*). A driving force greater than that required to initially place the sorbate in the micropore would then be required to remove the sorbate (i.e., a smaller relative pressure would be required to remove the sorbate compared to the initial sorption isotherm), leading to apparent hysteresis. Studies of trichloroethylene desorption from microporous mineral solids by Werth and Reinhard (*20*) and Farrell et al. (*21*) under near 100% relative humidity conditions support the hypothesis for this relatively hydrophilic solute. Huang et al. (*22*), however, have shown that sorption of phenanthrene to porous inorganic sorbents is characterized by relatively low sorption capacities due to preferential sorption of water on the hydrophilic surfaces of such sorbents, suggesting that sorption in the micropores of inorganic matrices is likely not a significant contributor to the observed desorption hysteresis of similarly hydrophobic solutes in saturated aqueous systems. Other explanations for nonartifactual desorption hsyteresis include a matrix change from the sorption cycle to the desorption cycle due to structural rearrangement of macromolecules in glassy regions of organic macromolecules (*23*, *24*).

The work described in this second of a series of papers on the subject focuses on developing an understanding of the fundamental mechanisms responsible for apparent hysteresis in the desorption of HOCs from NOM macromolecules. Through use of well-characterized natural and model organic sorbents under similar experimental conditions, investigation of the relative impacts of macromolecular mobility on sorption linearity and desorption hysteresis are qualitatively and quantifiably addressed. We begin with an examination of sorption isotherm linearity as a function of macromolecular mobility to further develop the foundation

* Corresponding author phone: (615)343-7070; fax: (615)322-3365; e-mail: eugene.j.leboeuf@vanderbilt.edu.
† Vanderbilt University.
‡ The University of Michigan.

10.1021/es991104g CCC: $19.00
Published on Web 07/29/2000

TABLE 1. NOM Isotherm Model Parameters

		Freundlich model			dual reactive domain model				linear model	
sorbent	N[a]	log K_F[b]	n[c]	R^2	K_D[d]	Q^o_a[e]	b[f]	R^2	K_D	R^2
cellulose	20	−0.183	1.025	0.999	NA[g]	NA	NA	NA	0.768	0.992
		(0.074)	(0.036)						(0.032)	
Lignin (Alkali)	20	1.320	0.804	0.999	0.000	12580	0.00073	0.996	7.048	0.991
		(0.106)	(0.054)		NA	(391.2)	(0.000)		(0.311)	
Aldrich Humic Acid	20	1.504	0.836	1.000	11.099	445.9	0.0402	0.998	12.48	0.995
		(0.028)	(0.015)		(0.844)	(310.7	(0.0592)		(0.42)	
Peat Humic Acid	20	1.289	0.787	1.000	3.91	655.6	0.0129	0.998	5.093	0.989
		(0.037)	(0.018)		(0.48)	(341.7)	(0.0116)		(0.251)	
Green River Kerogen	20	2.170	0.900	1.000	0.000	94720	0.0013	0.993	0.755	0.976
		(0.124)	(0.060)		NA	(4124)	(0.000)		(5.485)	
Ohio Shale II Kerogen	20	3.106	0.521	0.999	56.50	9373	0.0495	0.974	78.29	0.949
		(0.198)	(0.096)		(20.21)	(9789)	(0.151)		(8.34)	
Illinois No. 6 Coal	20	3.337	0.571	0.999	110.78	2267	0.0495	0.998	53.05	0.807
		(0.035)	(0.021)		(19.34)	(5037)	(0.0223)		(11.34)	
Wyoming Coal	20	2.807	0.624	1.000	40.84	11300	0.0212	0.998	66.81	0.965
		(0.032)	(0.016)		(6.60)	(3627)	(0.0132)		(5.84)	

[a] Number of observations. [b] K_F units are [μg/g][L/μg]^n, 95% confidence interval for log K_F in parentheses. [c] Freundlich exponent [-], 95% confidence interval in parentheses. [d] K_D units are [μg/g][L/μg], 95% confidence interval in parentheses. [e] Q^o_a units are [μg/g], 95% confidence interval in parentheses. [f] b units are [L/μg], 95% confidence interval in parentheses. [g] Not available.

TABLE 2. Synthetic Polymer Isotherm Model Parameters

		Freundlich model			dual reactive domain model				linear model	
sorbent	N[a]	log K_F[b]	n[c]	R^2	K_D[d]	Q^o_a[e]	b[f]	R^2	K_D	R^2
poly(butyl methacrylate)	20	1.960	1.046	0.999	NA	NA	NA	NA	124.0	0.959
		(0.098)	(0.066)						(11.8)	
poly(butyl/isobutyl methacrylate)	20	1.522	1.059	1.000	NA	NA	NA	NA	46.11	0.982
		(0.056)	(0.034)						(2.84)	
poly(isobutyl methacrylate)	20	1.323	1.045	1.000	NA	NA	NA	NA	26.32	0.993
		(0.033)	(0.022)						(1.03)	
poly(methyl methacrylate)	20	0.01016	0.840	1.000	0.259	55.92	0.00807	1.000	0.406	0.991
		(0.034)	(0.019)		(0.019)	(12.04)	(0.0013)		(0.018)	
poly(phenyl methacrylate)	20	2.840	0.573	1.000	33.99	7700	0.0458	0.999	63.19	0.948
		(0.044)	(0.026)		(4.17)	(1332)	(0.0176)		(6.77)	

[a] Number of observations. [b] K_F units are [μg/g][L/μg]^n, 95% confidence interval for log K_F in parentheses. [c] Freundlich exponent [-], 95% confidence interval in parentheses. [d] K_D units are [μg/g][L/μg], 95% confidence interval in parentheses. [e] Q^o_a units are [μg/g], 95% confidence interval in parentheses. [f] b units are [L/μg], 95% confidence interval in parentheses. [g] Not available.

of our work, followed with a detailed evaluation of potential mechanisms influencing observed desorption hysteresis. The third paper in this series investigates temperature and equilibration period effects on sorption and desorption behavior.

Materials and Methods

Sorbents. The general characteristics and preparation methods for the 14 natural and synthetic macromolecular sorbents used in this study were summarized in the first paper of this series (*25*).

Isotherms. (A) Chemicals. Spectrophotometric grade phenanthrene (98% Aldrich Chemical Co., Inc.) was used as the probe solute for both sorption and desorption isotherm measurements. Primary stock solutions of phenanthrene were prepared by dissolving an appropriate mass in methanol (HPLC grade, Fisher Scientific) and sequentially diluting with methanol to produce a range of stock solutions of various concentrations (e.g., 10, 100, and 1000 μg/L). Stock solutions were stored in a light-resistant box at −5 °C in 125 mL brown-colored glass bottles with aluminum crimp caps containing Teflon-lined silicone septa.

Aqueous solutions of phenanthrene comprised appropriate amounts of phenanthrene stock solution added to a buffered solution of double-distilled, filtered water (Nanopure, Barnsted Corporation) containing 0.005 M $CaCl_2$ and 100 mg/L NaN_3 (for biological control), buffered at pH 7 with $NaHCO_3$ (approximately 5.0 mg/L). Methanol concentrations within these solutions were maintained at less than 0.2 vol % in all experiments to reduce possible cosolvency effects (*26*).

(B) Analytical Methods. Aliquots of phenanthrene solution from initial (C_o) and final (following completion of the sorption/desorption experiment and suspension separation) aqueous supernatant ($C(t)$) solutions were immediately sampled and placed in 4-mL glass vials containing 2.00 mL of methanol (HPLC grade, Fisher Scientific), sealed with caps containing Teflon-lined septa, and stored at −5 °C. Samples from the 4 mL vials were transferred to 1.5 mL GC vials and analyzed using reverse-phase High-Pressure Liquid Chromatography (HPLC) (Prodigy 5 μm ODS(3) 100 Å, 100 × 2.00 mm column on a Hewlett-Packard (HP) Model 1050) equipped with a fluorescence detector (model HP 1046A), diode array detector (HP Series 1050), and 121 vial capacity autosampler. Using a modification of a method originally developed by Young (*27*), phenanthrene concentrations ranging from 0.5 to 1000 μg/L were mobilized in a mixture containing 90% acetonitrile (HPLC grade, Fisher Scientific) and 10% Nanopure water. Concentrations of 0.5 to 50 μg/L were detected by the fluorescence detector at 250-nm excitation wavelength and 364-nm emission spectra, and concentrations of 50 μg/L to 1000 μg/L were detected by the diode array detector using an ultraviolet (UV) spectra of 250-nm. External phenanthrene standards (in methanol) were

utilized to develop quadratic calibration curves for the fluorescence detector and linear calibrations for the diode array detector. Vial concentrations were determined by averaging triplicate injections of 15 μL of each, with a standard deviation of approximately 1−3%.

(C) Reactor Systems. All sorption and desorption experiments were conducted using completely mixed batch reactors (CMBRs). For equilibration periods of 42 days or less, 25 mL clear quartz glass centrifuge tubes (Kimax) and 40 mL clear borosillicate glass tubes (Wheaton) were used with sorbents possessing moderate sorption capacities (cellulose (25 mL tube), lignin, Aldrich humic acid, peat humic acid, and each of the synthetic polymers), and 125 mL narrow mouth amber glass bottles (Wheaton) were used with sorbents with high sorption capacities (Green River kerogen, Ohio Shale II kerogen, Illinois No. 6 coal, and Wyoming coal). Each bottle was sealed with screw caps with Teflon-lined silicone-backed septa and silver foil to minimize system losses to the Teflon liner. System losses were consistently less than 3.5% for each reactor system up to a period of 42 days. For equilibration periods exceeding 42 days, 20 mL (Kimble) or 50 mL prescored glass ampules (Wheaton) were used for sorbents with moderate or high sorption capacities, respectively.

(D) Sorption Experiments. Phenanthrene sorption isotherms were measured for 13 different sorbents at 25 ± 0.3 °C for equilibration periods of 355 days (except for Green River kerogen and Ohio Shale II kerogen, which were equilibrated for 90 days, and lignin (organosolv) which was equilibrated for 42 days). Rate of sorption studies conducted in parallel with these experiments suggested that these equilibration periods were sufficient to reach operational equilibrium for each sorbent. Isotherm points consisted of duplicate reactors dosed with an equivalent amount of sorbent, each equilibrated with initial aqueous phase phenanthrene concentrations spanning a range of approximately 5 μg/L to 1100 μg/L. A constant solids (sorbent) to solution ratio, adjusted to ensure 30−70% sorbate uptake, was used for all experiments 42 days and shorter, while studies lasting up to 355 days used a varying solids-to-solution ratio (greater sorbent dose at lower concentrations) to ensure approximately 40−60% sorbate uptake at equilibrium. Control reactors without sorbent were prepared in the same manner mentioned above. No corrections in isotherm calculations were required since average system losses to control reactors were consistently less than 3.5% of initial concentration. Additional experimental details are provided in ref *28*.

(D) Desorption Experiments. Desorption experiments were performed using either a single-cycle, withdraw-and-refill batch technique (Protocol I) similar to that developed in ref *12* or a single-cycle, withdraw-and-refill in a new bottle technique (Protocol II). Protocol I entailed the use of the same CMBR vessels for the desorption isotherm as that used for the initial sorption isotherm (i.e., for 42 days or less, 25 mL, 40 mL, or 125 mL bottles were used, while experiments lasting longer than 42 days were conducted in prescored glass ampules). After conducting a sorption isotherm experiment in the manner described above, approximately 80% of the remaining supernatant was removed from the reactor vessel, the vessel was reweighed, and an equal amount of phenanthrene-free buffered solution was added to the reactor. After a predetermined desorption period, separation of the solid phase from the aqueous phase and analysis of the supernatant were conducted in the same manner as used for the original sorption isotherm.

Development of Protocol II was deemed necessary for experiments involving use of synthetic polymers in glass ampule reactors (>42 day sorption periods). In these experiments, it was observed that some residual polymer often remained "stuck" to the ampule tip, thus preventing one from discarding the tip, and using the same ampule for

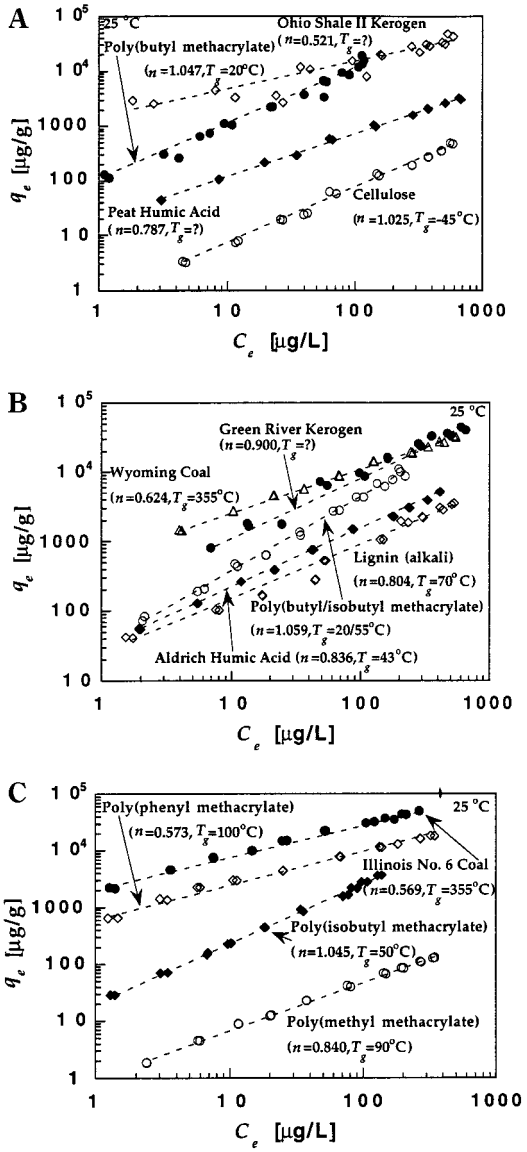

FIGURE 1. Freundlich model fits of phenanthrene sorption on (A) cellulose, Peat Humic Acid, poly(butyl methacrylate), and Ohio Shale II Kerogen; (B) Aldrich HA, Lignin, PBMA, Green River Kerogen, and Wyoming Coal; and (C) PMMA, PPMA, and Illinois No. 6 Coal.

desorption. To address this issue, the contents of each ampule were transferred to a 125 mL amber glass bottle (Wheaton) by pouring the contents into the bottle and rinsing the ampule four separate times with buffer solution. The ampule tip containing some of the "stuck" polymer was then placed inside the 125 mL bottle to ensure all original isotherm sorbent was contained within the "new" desorption reactor. The reactor was then backfilled with an appropriate amount of phenanthrene-free buffer solution. Again, after a predetermined desorption period, separation of the solid phase from the aqueous phase and analysis of the supernatant were conducted in a manner similar to that employed for the original sorption isotherm. Analysis of desorption data of controls using this technique showed no noticeable increase in desorption hysteresis compared to desorption experiments using Protocol I with 40 mL bottles.

Results and Discussion

Sorption Isotherms. In the first paper in this series (*25*), a more refined view of NOM was developed to encompass the inherent heterogeneity of natural organic matter as one

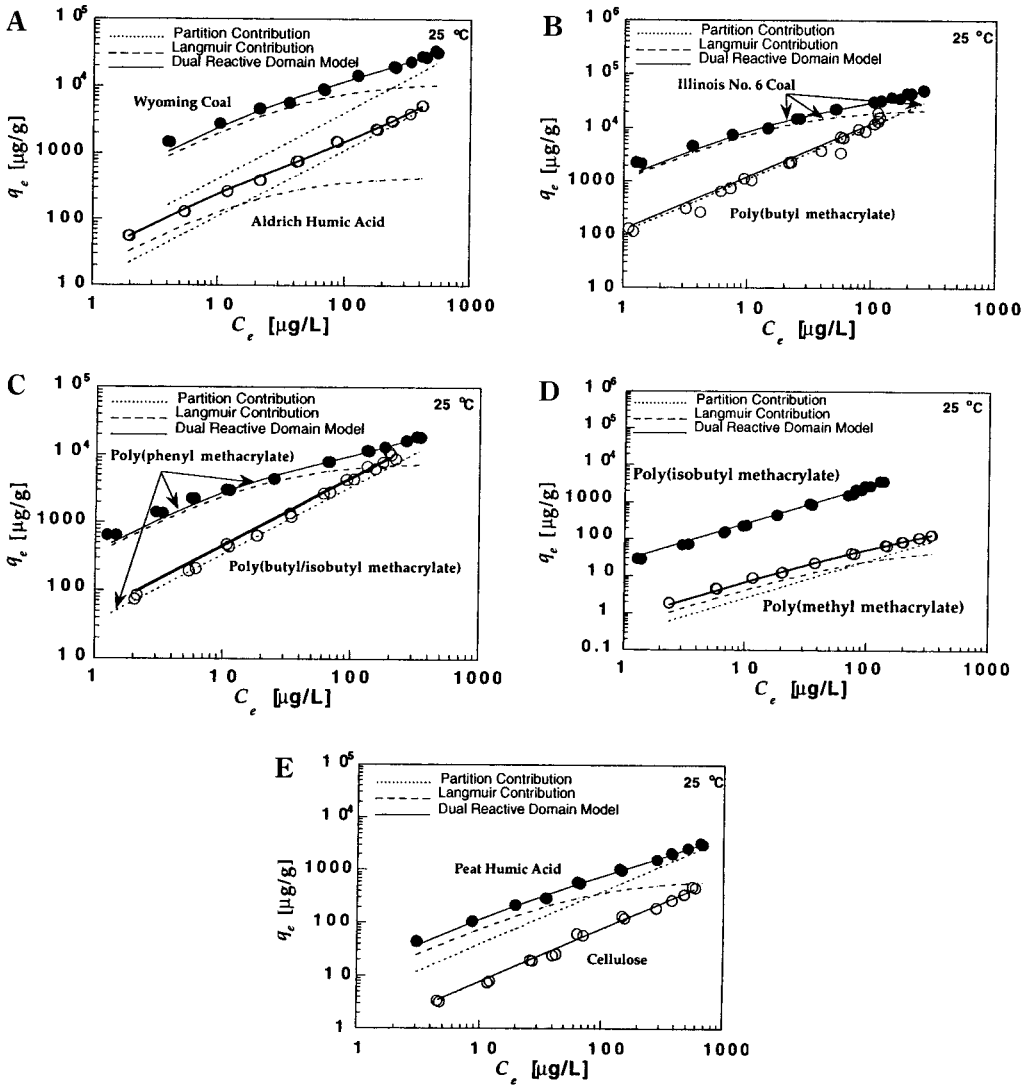

FIGURE 2. Dual reactive domain model fits of (A) Aldrich Humic Acid and Wyoming Coal; (B) PBMA and Illinois No. 6 Coal; (C) PBIMA and PPMA; (D) PMMA and PIMA; and (E) cellulose and Peat Humic Acid.

originating from a complex conglomeration of bits and pieces of degraded or partially degraded biopolymers that manifest themselves into mechanically different rubbery and glassy states. Sorption of HOCs from aqueous solution within these matrices has been characterized as both linear (e.g., refs *29*−*33*) and nonlinear sorption processes (e.g., refs *12*, *34*−*40*), and the relative nonlinearity of the sorption isotherm has been attributed to the presence of more condensed, diagenetically altered, glasslike regions of NOM (*12*, *25*, *37*−*45*) or similarly to microporous regions of carbonaceous (e.g., soot) materials in soils (*46*−*48*). In this section, we expand our database of observed nonlinear sorption in sorbents with known glass transition temperatures (T_g) in an effort to further establish the role of macromolecular mobility in influencing sorption isotherm linearity.

Sorption isotherms were modeled using a linear partitioning model, a log-linearized form of the Freundlich model noted in eq 1

$$\log q_e = \log K_F + n \log C_e \tag{1}$$

where q_e is the solid-phase concentration (μg/g), C_e is the aqueous-phase concentration (μg/L), K_F is the Freundlich capacity factor [(mg/L)(L/mg)^n], and n is the Freundlich exponent (unitless), and the Dual Reactive Domain Model (DRDM) (eq 2), comprising combined linear (partitioning) and nonlinear (adsorption) components

$$q_{e_T} = K_D C_e + \frac{Q_a^o b C_e}{1 + bC_e} \tag{2}$$

where K_D is the linear distribution coefficient [L^3/M]; Q_a^o represents the adsorbed phase solute concentration that corresponds to saturation of the glassy state [M/M]; and b is a coefficient related to the enthalpy of sorption in the glassy state [L^3/M]. Model parameters corresponding to 95% confidence intervals were determined using linear and nonlinear regression (utilizing either a Quasi-Newton or Simplex minimization search technique) with SYSTAT (version 5.2.1, SYSTAT, Inc.). Log-linearized Freundlich, Dual Reactive Domain, and linear isotherm model parameters for phenanthrene sorption on NOM and synthetic polymers are summarized in Tables 1 and 2, respectively. Figure 1 illustrates Freundlich model fits for each of the 13 sorbents, where the Freundlich n term is used to assess linearity/nonlinearity of the sorption isotherm, where linear sorption would be reflected by an n value of unity, while values of n lower than unity signify increasing heterogeneity of sites and increased sorption energies.

Several observations may be made from Tables 1 and 2 and Figure 1. First, known rubbery sorbents (i.e., those

TABLE 3. NOM Sorption and Desorption Isotherm Model Parameters and Hysteresis Indices

	sorption isotherm				desorption isotherm				hysteresis indices		
sorbent	log K_F[a]	n[b]	R^2	N[c]	log K_F	n	R^2	N	C_e = 1 [μg/L]	C_e = 10 [μg/L]	C_e = 100 [μg/L]
cellulose	−0.183	1.025	0.999	20	−0.572	1.156	0.995	20	0.196	0.132	0.071
	(0.074)	(0.036)			(0.146)	(0.080)					
Aldrich Humic Acid	1.504	0.836	1.000	20	1.3912	0.893	1.000	20		0.029	0.153
	(0.028)	(0.015)			(0.042)	(0.025)					
Peat Humic Acid	1.289	0.787	1.000	20	1.146	0.880	1.000	20		0.015	0.183
	(0.037)	(0.018)			(0.057)	(0.032)					
Green River Kerogen	2.550	0.788	1.000	22	2.176	0.939	0.997	20			-
	(0.087)	(0.045)			(0.22)	(0.128)					
Ohio Shale II Kerogen	3.164	0.548	1.000	22	3.173	0.599	1.000	22	0.261	0.368	0.484
	(0.026)	(0.049)			(0.048)	(0.029)					
Illinois No. 6 Coal	3.337	0.571	1.000	20	3.347	0.640	1.000	20	0.171	0.316	0.479
	(0.035)	(0.021)			(0.039)	(0.028)					
Wyoming Coal	2.807	0.624	1.000	20	2.784	0.683	1.000	20	0.254	0.274	0.295
	(0.032)	(0.016)			(0.049)	(0.029)					

[a] K_F units are [μg/g][L/μg]^n, 95% confidence interval for log K_F in parentheses. [b] Freundlich exponent [-], 95% confidence interval in parentheses. [c] Number of observations.

TABLE 4. Synthetic Polymer Sorption and Desorption Isotherm Model Parameters and Hysteresis Indices

	sorption isotherm				desorption isotherm				hysteresis indices		
sorbent	log K_F[a]	n[b]	R^2	N[c]	log K_F	n	R^2	N	C_e = 1 [μg/L]	C_e = 10 [μg/L]	C_e = 100 [μg/L]
poly(butyl methacrylate)	1.960	1.047	0.999	20	1.974	0.991	0.999	20	0.061	0.022	-
	(0.098)	(0.066)			(0.076)	(0.052)					
poly(butyl/isobutyl methacrylate)	1.52196	1.059	1.000	20	1.715	1.005	0.999	20	0.419	0.522	0.633
	(0.056)	(0.034)			(0.120)	(0.078)					
poly(isobutyl methacrylate)	1.323	1.04453	1.000	20	1.725	0.987	0.999	18	2.368	2.419	2.470
	(0.033)	(0.022)			(0.091)	(0.077)					
poly(methyl methacrylate)	0.010	0.840	1.000	20	0.304	0.821	0.998	16	0.523	0.717	0.937
	(0.034)	(0.019)			(0.083)	(0.061)					
poly(phenyl methacrylate)	2.841	0.573	1.000	20	2.828	0.623	1.000	18	0.873	0.941	1.012
	(0.044)	(0.026)			(0.054)	(0.036)					

[a] K_F units are [μg/g][L/μg]^n, 95% confidence interval for log K_F in parentheses. [b] Freundlich exponent [-], 95% confidence interval in parentheses. [c] Number of observations.

sorbents with "water-wet" glass transition temperatures (T_g's) close to or below the experimental temperature) cellulose, PBMA, and PBIMA exhibit linear sorption. Only PIMA, with a water-wet T_g of 50 °C exhibits linear sorption at a temperature distinctly different from its "water-wet" T_g. Second, known glassy sorbents lignin (alkali) (assuming lignin (organosolv) T_g is representative of the alkali T_g), PMMA, PPMA, Illinois No. 6 coal, and Wyoming coal all illustrate nonlinear sorption at the 95% confidence interval. Third, the higher the T_g is relative to the experimental temperature, the more nonlinear the sorption, as evidenced by greater nonlinearity in the coals ($T_g \cong$ 355 °C) versus PPMA (T_g = 100 °C), PMMA (T_g = 90 °C), and lignin (T_g = 70 °C). Fourth, in agreement with results reported by ref *45* sorption capacities (as measured by K_F) changed as an apparent function of the age of the natural organic matter; from relatively low capacities within the biopolymers, to increased capacities within diagenetically altered peat and Aldrich humic acid, and greatest capacities within the most digenetically advanced sorbents (kerogens and coals). Fifth, the linear sorption model appears only to be applicable to sorbents in the rubbery state. Glassy sorbents displaying nonlinear sorption behavior are clearly not fit well by the linear sorption model.

The relative contribution of the hypothesized immobilized regions present within glassy matrices to overall sorption isotherm linearity/nonlinearity is best illustrated through use of the DRDM introduced by LeBoeuf and Weber (*41*). The results are presented in Figure 2 and summarized in Tables 1 and 2. As expected, nonlinear contributions to sorption are significant for the glassy sorbents; only the partitioning component is present for the rubbery sorbents.

Figure 2A shows DRDM fits of Aldrich humic acid and Wyoming coal. Aldrich humic acid, with a water-wet T_g of 43 °C illustrates a relatively large partitioning contribution to overall sorption compared to the partitioning contribution of Wyoming coal ("dry" $T_g \cong$ 350 °C (estimated from ref *49*)). Additionally, the lower Langmuir sorption capacity of Aldrich humic acid results in greater partitioning contributions at lower solid-phase loading relative to the adsorption component, while very large sorbed phase loadings are required for dominance of the partitioning process within Wyoming coal. Figure 2B−D illustrates respective DRDM plots of glassy Illinois No. 6 coal ("dry" $T_g \cong$ 355 °C (estimated from ref *49*); unknown water-wet T_g) and rubbery PBMA ("dry" T_g = 29 °C; water wet T_g < 20 °C); glassy PPMA ("dry" T_g = 110 °C; water wet T_g = 100 °C) apparently rubbery PBIMA ("dry" T_g = 29/55 °C; water wet T_g = <20/50 °C); glassy PMMA ("dry" T_g = 105 °C; water wet T_g = 90 °C) and apparently rubbery PIMA ("dry" T_g = 55 °C; water wet T_g = 50 °C). These three plots provide for clear delineation of the relative contribution of the adsorption component to overall isotherm nonlinearity for glassy sorbents in contrast to rubbery matrices. The apparent discrepancy for the observed linear sorption in PBIMA and PIMA may be due to swelling of the matrix from sorbed phenanthrene and possible reversion of the PIMA T_g to values at or below the experimental temperature. DRDM fits for peat humic acid ("dry" T_g = 63 °C; unknown water wet T_g (*50*)) and cellulose ("dry" T_g = 225 °C; water wet T_g = −45 °C (*51*)) depicted in Figure 2E shows a

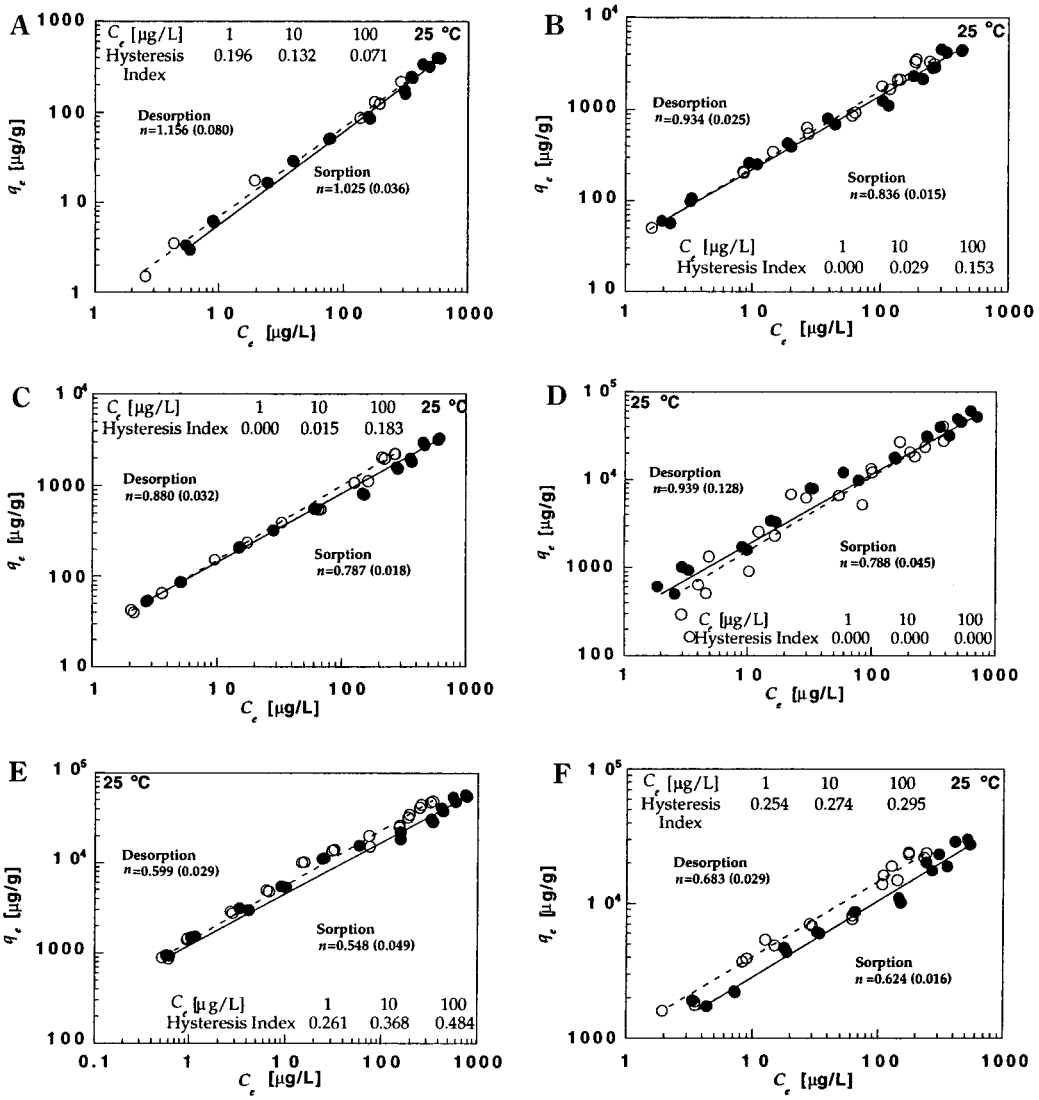

FIGURE 3. Sorption/desorption isotherms of (A) cellulose; (B) Aldrich humic acid; (C) Peat humic acid; (D) Green River Shale kerogen; (E) Ohio Shale II kerogen; and (F) Wyoming coal. Sorption isotherm data is characterized by dark circles; desorption data by light circles.

similar trend to that observed in Figure 2B–D.

A significant feature of the DRDM consistent with each glassy sorbent is the leveling-off of the nonlinear component at increased sorbed-phase concentrations, whereas the partitioning component continues to increase in relative contribution to the overall sorption isotherm. In fact, at large sorbed-phase concentrations, the isotherm is dominated by the partitioning process (e.g., see last eight data points for Aldrich humic acid in Figue 2A). This phenomenon may be explained in terms of an apparent limitation of available adsorption sites (i.e., through filling of surface adsorption sites and/or filling of meso- and micropores present within the immobilized regions of the glassy matrix), coupled with a possible increase in the partitioning domain due to additional solute uptake within the matrix, resulting in increased molecular mobility. One may thus envision a sorbent that may exhibit a sorption isotherm ranging from linear behavior (at very low, Henry's-Law range sorbed phase concentrations), to nonlinear behavior dominated by filling of relatively high energy adsorption sites, to more linear behavior as adsorption sites and/or micropores are filled, and increased sorbed phase activity of the sorbate results in increased regions of molecular mobility (swelling).

Desorption Isotherms. Desorption experiments presented in this study used a 90 day sorption period, followed by 28 day (for cellulose, Aldrich humic acid, peat humic acid, and all synthetic polymers) or 42 day (for Green River kerogen, Ohio Shale II kerogen, Illinois No. 6 coal, and Wyoming coal) desorption period. Each set of experiments was fit to the Freundlich isotherm equation (eq 1) using SYSTAT (version 5.2.1, SYSTAT Corp.) and consequently employed in eq 3 to quantify the desorption hysteresis index. Desorption hysteresis, defined at constant temperature and residual aqueous phase concentration (*12*), is given by

$$\text{desorption hysteresis} = \frac{q_e^d - q_e^s}{q_e^s}\Big|_{T,C_e} \qquad (3)$$

where q_e^d is the solid-phase sorbate concentration for single-cycle desorption [μg/g]; q_e^s is the solid-phase sorbate concentration for sorption isotherm [μg/L]; T is the absolute temperature [K]; and C_e is the aqueous phase concentration of sorbate [μg/L]. As noted by Huang et al. (*14*), this equation has advantages over the measure of hysteresis via the method of DiToro and Horzempa (*2*) in which the difference in the sorption and desorption distribution coefficients for a single reactor is used. Equation 3 utilizes data points from the entire sorption and desorption isotherm, and it incorporates influences of nonlinearity into the reported results.

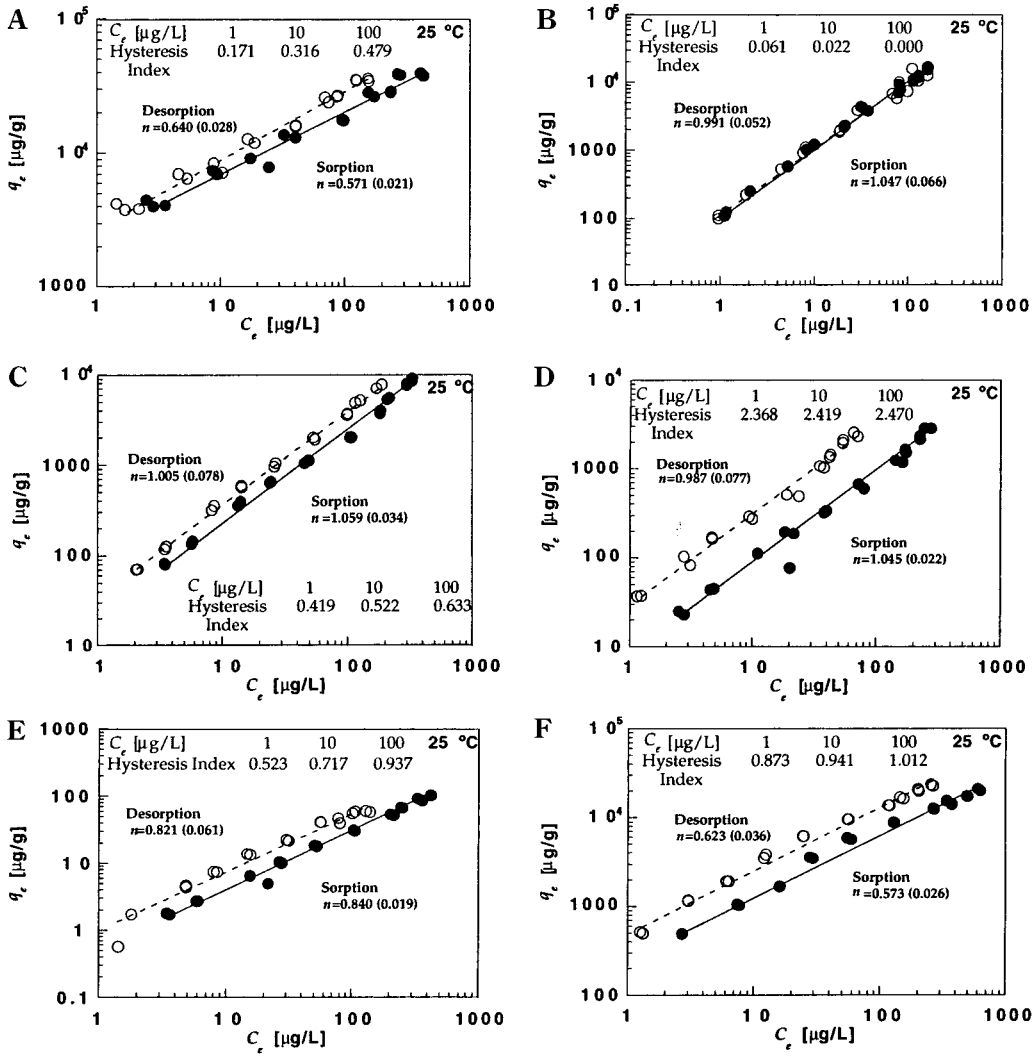

FIGURE 4. Sorption/desorption isotherms of (A) Illinois No. 6 coal; (B) PBMA; (C) PBIMA; (D) PIMA; (E) PMMA; and (F) PPMA.

Tables 3 and 4 provide summaries of the sorption/desorption experiments for seven natural organic matter samples (cellulose, Aldrich humic acid, peat humic acid, Green River kerogen, Ohio Shale II kerogen, Illinois No. 6 coal, and Wyoming coal) and five synthetic polymer samples (PBMA, PBIMA, PIMA, PMMA, and PPMA). Illustrations of each experiment are provided in Figures 3 and 4. For comparative purposes, Hysteresis Indices (H.I.s) were calculated based on 1, 10, and 100 μg/L phenanthrene concentrations in the aqueous phase and are noted in each table and on the respective figure for each sorbent. Evaluating H.I. at different aqueous phase concentrations provides additional insights into the relative influence concentration of the sorbing solute has on overall hysteretic behavior.

Examination of the above experimental results reveals that (i) younger (less diagenetically altered) natural sorbents (cellulose, Aldrich humic acid, and peat humic acid) generally exhibited less desorption hysteresis compared to more diagenetically altered sorbents (Ohio Shale II kerogen, Illinois No. 6 coal, and Wyoming coal); (ii) desorption hysteresis appears to be a function of the sorbent's glass transition temperature (i.e., sorbents at or near their rubbery state (cellulose, Aldrich humic acid, and PBMA) tend to show little to no desorption hysteresis, while sorbents in the glassy state tend to show relatively larger desorption hysteresis indices); (iii) desorption isotherms for natural sorbents tend to be more linear (as measured by the Freundlich exponent, n) compared to the sorption isotherm, while the difference in desorption isotherm linearity for the synthetic polymers was either similar to (PPMA) or opposite (PBIMA, PIMA, and PMMA) that observed for natural sorbents; and (iv) isotherm linearity is not a definitive predictor of hysteresis indices (e.g., Green River kerogen, PBIMA, and PIMA).

The trend for increased desorption hysteresis with increased diagenetic alteration generally follows similar insightful observations made by Huang et al. (*12*) and Weber et al. (*13*) for desorption of phenanthrene from natural soils and sediments. The more polar nature of younger NOMs (primarily consisting of oxygen-substituted functional groups such as carboxyl, carbonyl, and hydroxyl) facilitates greater hydrophilic interactions, resulting in greater swelling of these matrices, relative to their hydrophobic counterparts. In fact this trend also holds true for highly diagenetically altered NOM, where Wyoming coal (O/C = 0.24) is less hysteretic than Illinois No. 6 coal (O/C = 0.17). However, the O/C correlation does not explain the absence of desorption hysteresis in Green River kerogen (O/C ratio of 0.19) compared to the observed hysteresis in more diagenetically altered Ohio Shale II (O/C = 0.23). It is possible that the increased aromatic carbons observed in the ^{13}C NMR spectra of Ohio Shale II (characterized in the first paper in this series (*25*) are actually imposing specific regions of molecular immobility, compared to Green River kerogen with ^{13}C NMR spectra revealing the presence of only aliphatic carbon chains, which are likely more mobile in aqueous solution. Additionally, PBMA (water-wet T_g < 20 °C, O/C ratio of 0.33),

which is much more hydrophobic than PMMA (O/C ratio of 0.53), and is thus expected to sorb comparatively less water, shows no desorption hysteresis, while PMMA (water-wet T_g = 90 °C) exhibits considerable hysteresis. A related, but more logical explanation than the O/C ratio may reside in the actual macromolecular mobility of the sorbent matrix, and its ability to quickly accommodate sorbing or desorbing solutes.

As noted above, sorbents with known glass transition temperatures residing in the rubbery state at 25 °C (cellulose and PBMA) exhibited little to no desorption hysteresis, while all glassy sorbents displayed some form of desorption hysteresis. As such, there appears to be a general, qualitative trend of the H.I. as a function of a sorbent's system-specific T_g (taking into account the experimental temperature, and relative uptake of water and sorbate within the sorbing matrix). As noted above, the decreased desorption hysteresis in rubbery systems may be primarily attributed to relatively faster rates of sorption (and subsequent desorption) from the matrix. An initial indicator that nonequilibrium, as opposed to micropore filling, is playing a dominant role in observed desorption hysteresis for sorbents near their glass transition temperature may be evidenced by observations of linear isotherms for PBIMA and PIMA, but significant desorption hysteresis. Additionally, attempts to correlate CO_2-based micropore capacity with H.I. (detailed in forthcoming paper 4 of this series) returned relatively poor correlation coefficients, primarily due to the lack of desorption hysteresis for Green River kerogen, a sorbent with high micropore volume. Other sorbents with high T_g's relative to the experimental temperature, however, tended to show at least a qualitative trend of increasing H.I. with micropore capacity. It is possible, however, that the behavior of Green River kerogen may be explained by the presence of larger, less restrictive micropores compared to more diagenetically altered NOMs.

The general trend for greater desorption isotherm linearity compared to the sorption isotherm, although not statistically significant at the 95% confidence level in all cases, may be explained in similar terms to hysteresis in synthetic polymeric systems (*23, 24*). Larger sorbed-phase concentrations result in increased irreversible swelling compared to lower sorbed-phase concentrations. Upon exposure to the decreased concentrations present in the desorption cycle, the sorbent matrix thus remains in a more swollen condition than what would be thermodynamically predicted based solely on the hypothesis of reversible swelling during the sorption isotherm. Additional sorption sites are therefore available for sorption. PPMA follows a similar trend as NOMs, although PMMA, PIMA, and PBIMA do not. Reasons for the change in linearity for the glassy PMMA may be associated with the low HOC affinity of PMMA, possibly leading to the combined effects of reduced swelling-induced macromolecular rearrangement and slower rates of sorption. As observed in ref *28*, and as will be reported in forthcoming papers in this series, increased equilibration periods generally result in decreased isotherm linearity for those glassy sorbents not yet reaching equilibrium. This phenomenon may also be applicable to the sorption behavior observed in PIMA and PBIMA. Evaluation of temperature effects and equilibration period on desorption behavior in the following paper in this series provide additional insights into the relative impacts of macromolecular mobility and nonequilibrium sorption behavior on desorption hysteresis.

Acknowledgments

We thank Colleen O'Brien, Kai Kuo, Christopher Meinke, David Peevers, and Jung (Josh) Suh for their assistance with the experimental aspects of this work. This research was funded in part by the Great Lakes and Mid-Atlantic Center for Hazardous Substance Research R2D2 Program under a grant from the Office of Research and Development, U.S. Environmental Protection Agency. Partial funding of the research activities of the Center is also provided by the State of Michigan Department of Environmental Quality. The content of this publication does not necessarily represent the views of either agency. Partial support was also provided by a University of Michigan Regents Fellowship award to E.J.L. We also note our gratitude to three anonymous reviewers for their helpful remarks.

Literature Cited

(1) Karickhoff, S. W. *Chemosphere* **1981**, *10*, 833−846.
(2) Di Toro, D. M.; Horzempa, L. M. *Environ. Sci. Technol.* **1982**, *16*, 594−602.
(3) Horzempa, L. M.; DiToro D. M.*Water Res.* **1983**, *17*, 851−859.
(4) Oliver, B. G. *Chemosphere* **1985**, *14*, 1087−1106.
(5) Steinberg, S. M.; Pignatello, J. J.; Sawhney, B. L. *Environ. Sci. Technol.* **1987**, *21*, 1201−1208.
(6) Pignatello, J. J. *Environ. Toxicol. Chem.* **1990**, *9*, 1107−1115.
(7) Pignatello, J. J. *Environ. Toxicol. Chem.* **1990**, *9*, 1116−1126.
(8) Pignatello, J. J.; Huang, L. Q. *J. Environ. Quality* **1991**, *20*, 222−228.
(9) Kan, A. T.; Fu, G.; Hunter, M. A.; Tomson, M. B. *Environ. Sci. Technol.* **1997**, *31*, 2176−2185.
(10) Hatzinger, P. B.; Alexander, M. *Environ. Sci. Technol.* **1995**, *29*, 537−545.
(11) Bhandari A.; Novak, J. T.; Burgos, W. D.; Berry, D. F. *J. Environ. Eng.* **1997**, *123*, 506−513.
(12) Huang, W.; Yu, H.; Weber, W. J., Jr. *J. Contam. Hydrology* **1998**, *31*, 129−148.
(13) Weber, W. J., Jr.; Huang, W.; Yu H. *J. Contam. Hydrology* **1998**, *31*, 149−165.
(14) Huang, W.; Yu, H.; Weber, W. J., Jr. *Environ. Sci. Technol.* **1997**, *31*, 2562−2569.
(15) Burgos, W. D.; Novak, J. T.; Berry, D. F. *Environ. Sci. Technol.* **1996**, *30*, 1205−1211.
(16) Ball, W. P.; Roberts, P. V. In *Organic Substances and Sediments in Water*; Lewis Publishers: Chelsea, MI, 1991; p 273.
(17) Harmon, T. C.; Roberts, P. V. *Water Sci. Technol.* **1992** *26*, 71−77.
(18) Farrell, J.; Reinhard, M. *Environ. Sci. Technol.* **1994**, *28*, 53−62.
(19) Gregg, S. J.; Sing, K. S. W. *Adsorption, Surface Area, and Porosity*, 2nd ed.; Academic Press: New York, 1982.
(20) Werth, C. J.; Reinhard, M. *Environ. Sci. Technol.* **1997**, *31*, 697−703.
(21) Farrell, J.; Grassian D.; Jones M. *Environ. Sci. Technol.* **1999**, *33*, 1237−1243.
(22) Huang, W.; Schlautman, M. A.; Weber, W. J., Jr. *Environ. Sci. Technol.* **1996**, *30*, 105−113.
(23) Crank, J.; Park, G. S. In *Diffusion in Polymers;* Academic Press: New York, 1968.
(24) Vrentas, J. S.; Vrentas, C. M. *Macromolecules* **1996**, *29*, 4341−4396.
(25) LeBoeuf, E. J.; Weber, W. J., Jr. *Environ. Sci. Technol.* **2000**, *34*, 3623−3631.
(26) Wauchope, R. D.; Savage, K. E.; Koskinin, W. C. *Weed Sci.* **1983**, *31*, 744−751.
(27) Young, T. M. Ph.D. Dissertation, The University of Michigan, Ann Arbor, MI, 1995.
(28) LeBoeuf, E. J. Ph. D. Dissertation, The University of Michigan, Ann Arbor, MI, 1998.
(29) Chiou, C. T.; Peters, L. J.; Freed, V. H. *Science* **1979**, *206*, 831−832.
(30) Karickoff, S. W.; Brown, D. S.; Scott, T. A. *Water Res.* **1979**, *13*, 241−248.
(31) Schwarenbach, R. P.; Westall, J. *Environ. Sci. Technol.* **1981**, *15*, 1360−1367.
(32) Kile, D. E.; Chiou, C. T.; Li, H.; Xu, O. *Environ. Sci. Technol.* **1995**, *29*, 1401−1406.
(33) Chin, Y. P.; Weber, W. J., Jr. *Environ. Sci. Technol.* **1989**, *23*, 978−984.
(34) Miller, C. T.; Weber, W. J., Jr. *Environ. Sci. Technol.* **1986**, *31*, 243−261.
(35) Weber, W. J., Jr.; McGinley P. M.; Katz, L. E. *Environ. Sci. Technol.* **1992**, *26*, 1955−1962.
(36) Spurlock, F. C.; Biggar, J. E. *Environ. Sci. Technol.* **1994**, *28*, 996−1002.
(37) Young, T. M.; Weber, W. J., Jr. *Environ. Sci. Technol.* **1995**, *29*, 92−97.

(38) Weber, W. J., Jr.; Huang, W. *Environ. Sci. Technol.* **1996**, *30*, 881−888.
(39) Xing, B.; Pignatello J. J.; Gigliotti, B. *Environ. Sci. Technol.* **1996**, *30*, 2432−2440.
(40) Xing, B.; Pignatello, J. J. *Environ. Sci. Technol.* **1997**, *31*, 792−799.
(41) LeBoeuf, E. J.; Weber, W. J., Jr. *Environ. Sci. Technol.* **1997**, *31*, 1697−1702.
(42) LeBoeuf, E. J.; Weber, W. J., Jr. *Environ. Toxic., Chem.* **1999**, *18*, 1617−1626.
(43) LeBoeuf, E. J. *Environ. Sci. Technol.* **1999**, *33*, 2833−2834.
(44) LeBoeuf, E. J.; Weber, W. J., Jr. In *Proceedings of the 9th International Meeting of the Humic Substances Society*; 1999, In press.
(45) Huang, W.; Young, T. M.; Schlautman, M. A.; Weber, W. J., Jr. *Environ. Sci. Technol.* **1997**, *31*, 1703−1710.
(46) Xia, G. S.; Ball, W. P.. *Environ. Sci. Technol.* **2000**, *34*, 1246−1253.
(47) Chiou, C. T.; Kile, D. E.; Rutherford, D. W.; Sheng, C. Y.; Boyd, S. A. *Environ. Sci. Technol.* **2000**, *34*, 1255−1258.
(48) Karapanagioti, H. K.; Kleineidam, S.; Sabatini, D. S.; Grathwohl, P.; Ligous, B. *Environ. Sci. Technol.* **2000**, *34*, 406−414.
(49) Lucht, L. M.; Larson, J. M.; Peppas, N. A. *Energy Fuels* **1987**, *1*, 56−58.
(50) Young, K. D.; LeBoeuf, E. J. *Environ. Sci. Technol.* **2000**, *34*, In press.
(51) Akim, E. L. *Chemtech* **1978**, *8*, 676−682.

Received for review September 27, 1999. Revised manuscript received May 15, 2000. Accepted May 16, 2000.

ES991104G